EPJ Web of Conferences **137**, 06020 (2017) DOI: 10.1051/epjconf/201713706020
XIIth Quark Confinement & the Hadron Spectrum

Phenomenology of near-threshold states: a practical parametrisation for the line shapes

F.-K. Guo[1,2], C. Hanhart[3], Yu. S. Kalashnikova[4,5], P. Matuschek[3], R.V. Mizuk[6,5,7], A. V. Nefediev[4,5,7,a], Q. Wang[2,3], and J.-L. Wynen[3]

[1] *State Key Laboratory of Theoretical Physics, Institute of Theoretical Physics, Chinese Academy of Sciences, Beijing 100190, China*
[2] *Helmholtz-Institut für Strahlen- und Kernphysik and Bethe Center for Theoretical Physics, Universität Bonn, D-53115 Bonn, Germany*
[3] *Forschungszentrum Jülich, Institute for Advanced Simulation, Institut für Kernphysik (Theorie) and Jülich Center for Hadron Physics, D-52425 Jülich, Germany*
[4] *Institute for Theoretical and Experimental Physics, 117218, B.Cheremushkinskaya 25, Moscow, Russia*
[5] *National Research Nuclear University MEPhI, 115409, Kashirskoe highway 31, Moscow, Russia*
[6] *Lebedev Physics Institute, 119991, Leninsky prospect 53, Moscow, Russia*
[7] *Moscow Institute of Physics and Technology, 141700, 9 Institutsky lane, Dolgoprudny, Moscow Region, Russia*

Abstract. In the last decade many states in the spectrum of charmonium and bottomonium have been observed experimentally above the lowest open-flavour threshold. Most of these states reside in the vicinity of strong thresholds and show properties that cannot be captured by simple quark models. Description and understanding of such exotic states is a challenge for the phenomenology of strong interactions, since it requires building adequate theoretical tools and approaches. In this work, a practical parametrisation for the line shapes of near threshold resonance(s) is derived in the framework of a coupled-channel model which includes an arbitrary number of elastic and inelastic channels as well as of bare pole terms. Parameters of the distribution have a direct relation to phenomenology and the resulting analytical parametrisation is therefore ideally suited to harvest the full information content provided by the measurements and to establish a link between the experimental data and their theoretical interpretation.

1 Introduction

In 2003 the Belle Collaboration reported the observation of the state $X(3872)$ in the spectrum of charmonium [1] which could not be described in the framework of simple quark models. Since then the number of confirmed "homeless" charmonia and bottomonia exceeds a dozen, and most of them reside in the vicinity of strong S-wave thresholds which therefore play an important role for the properties of these exotic resonances. Another important feature of those states is that they are typically observed in both open- and hidden-flavour channels. Since high-precision and high-statistics data are expected

[a] e-mail: nefediev@itep.ru

to arrive soon from the new upcoming experiments [2–5] the task of building adequate approaches for the data analysis for exotic states becomes urgent.

It has to be noticed that the traditional way to perform a data analysis—employing sums of Breit-Wigner distributions for each peak combined with suitable background functions—meets severe difficulties. On one hand, in the Breit-Wigner formula, the loop operator is substituted by a constant width that makes it impossible as a matter of principle to address threshold phenomena in such an approach. On the other hand, the standard notions of the "mass" and the "width" inherent to the Breit-Wigner form may appear completely misleading for near-threshold resonances—this is probably best illustrated by the observation that although the data for the Z_b states have peaks above the $B^{(*)}\bar{B}^*$ thresholds they are compatible with bound state poles as soon as the energy dependence of the selfenergy of the states is included properly [6]. In addition, the Breit-Wigner formula violates analyticity, for it only account for a single pole in the amplitude. Furthermore, such an approach provides only limited information on the states studied, since the Breit-Wigner parameters are reaction-dependent and the naive algebraic sum of the Breit-Wigner distributions violates unitary. Finally, analysing each reaction channel individually, one does not exploit the full information content provided by the measurements.

We propose an alternative approach which provides an important link between various models and first-principles calculations in QCD (such as lattice simulations) from one side and the experimental data on the other side. In particular, we build a model-independent parametrisation for near-threshold states consistent with all requirements from unitarity and analyticity. The formulae derived are well suited for a simultaneous analysis of the entire bulk of data for all production and decay channels for the given near-threshold state(s). The parameters used possess a direct physical meaning and can be evaluated in microscopic approaches to QCD.

2 Coupled-channel problem

The approach is based on a coupled-channel model formulated in terms of the Lippmann-Schwinger equations for the t matrix. The interaction potential is taken in the form [7, 8]

$$\hat{V} = \begin{array}{c} \begin{matrix} b=\overline{1,N_{\rm p}} & \beta=\overline{1,N_{\rm e}} & i=\overline{1,N_{\rm in}} \end{matrix} \\ \begin{pmatrix} v_{ab} & v_{a\beta}(\boldsymbol{p}') & v_{ai}(\boldsymbol{k}) \\ v_{\alpha b}(\boldsymbol{p}) & v_{\alpha\beta}(\boldsymbol{p},\boldsymbol{p}') & v_{\alpha i}(\boldsymbol{p},\boldsymbol{k}) \\ v_{jb}(\boldsymbol{k}') & v_{j\beta}(\boldsymbol{k}',\boldsymbol{p}') & v_{ji}(\boldsymbol{k}',\boldsymbol{k}) \end{pmatrix} \end{array} \begin{array}{l} a=\overline{1,N_{\rm p}} \\ \alpha=\overline{1,N_{\rm e}} \\ j=\overline{1,N_{\rm in}}. \end{array} \tag{1}$$

Matrix (1) contains various types of interactions between $N_{\rm p}$ bare poles (describing quark states and labelled by latin letters a, b, c, and so on), N_e elastic open-flavour channels $(Q\bar{q})(q\bar{Q})$ (here Q and q denote the heavy and the light quark, respectively), and N_{in} inelastic hidden-flavour channels $(Q\bar{Q})(q\bar{q})$, labelled by greek letters α, β, γ, and so on and by latin letters i, j, k, and so on, respectively.

To proceed with an analytical solution of the Lippmann-Schwinger equations the transition potentials between the elastic and inelastic channels are assumed to take a separable form,

$$v_{\alpha i}(\boldsymbol{p},\boldsymbol{k}) = \chi_{i\alpha}(\boldsymbol{p})\varphi_{i\alpha}(\boldsymbol{k}). \tag{2}$$

It is obvious that the definition of Eq. (2) is invariant under the transformation

$$\chi_{i\alpha}(\boldsymbol{p}) \to C\chi_{i\alpha}(\boldsymbol{p}), \quad \varphi_{i\alpha}(\boldsymbol{k}) \to \varphi_{i\alpha}(\boldsymbol{k})/C, \tag{3}$$

with an arbitrary, real constant C, so that without loss of generality one can set

$$\chi_{i\alpha}(\boldsymbol{p} = 0) = 1. \tag{4}$$

In addition, it is quite natural to assume that $\chi_{i\alpha}$ is independent of i, since the transition of the open-flavour channels to the hidden-flavour channels demands the exchange of a heavy meson and therefore it is of a short-range nature for all inelastic channels as long as these channels are far from the thresholds of the elastic channels (so that the exchanged heavy meson is far off shell). Therefore, finally, one arrives at a vertex in the form

$$v_{\alpha i}(\boldsymbol{p}, \boldsymbol{k}) = \chi_\alpha(\boldsymbol{p})\varphi_{i\alpha}(\boldsymbol{k}). \tag{5}$$

It should also be noticed that the direct interaction potentials in the inelastic channels $v_{ji}(\boldsymbol{k}', \boldsymbol{k})$ can typically be neglected since they must be described either by isospin-violating short-range interactions (for example, by $\rho J/\psi \leftrightarrow \omega J/\psi$ for the $X(3872)$ in the spectrum of charmonium) or by pion exchanges between heavy quarkonia (for example, $\pi\Upsilon(nS)(\pi h_b(mP)) \leftrightarrow \pi\Upsilon(n'S)(\pi h_b(m'P))$ for the $Z_b(10610)$ and $Z_b(10650)$ in the spectrum of bottomonium) which only appear in higher orders of the chiral Lagrangian.

The two above assumptions about the separable form of the elastic-to-inelastic potential and about the negligibility of the direct interactions in the inelastic channels allow one to simplify the problem considerably. In particular, the inelastic channels can be completely disentangled from the elastic channels and from the quark states and they enter additively thus "dressing" other potentials and vertices with the inelastic loops,

$V_{ab} =$  , (6)

$V_{\alpha a}(\boldsymbol{p}) =$  , (7)

$V_{\alpha\beta}(\boldsymbol{p}) =$ 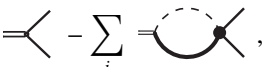 , (8)

$V_{\alpha\beta}(\boldsymbol{p}, \boldsymbol{p}') =$ 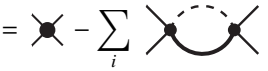 , (9)

where for the line definitions see the caption of Fig. 1.

Furthermore, using the approach of Refs. [9, 10], one can further disentangle the elastic channels from the bare poles, so that the only Lippmann-Schwinger equation to be solved is the equation for the elastic t matrix,

$$t_{\alpha\beta}(\boldsymbol{p}, \boldsymbol{p}') = V^{\text{eff}}_{\alpha\beta}(\boldsymbol{p}, \boldsymbol{p}') - \sum_{\gamma=1}^{N_\text{e}} \int V^{\text{eff}}_{\alpha\gamma}(\boldsymbol{p}, \boldsymbol{q}) S_\gamma(\boldsymbol{q}) t_{\gamma\beta}(\boldsymbol{q}, \boldsymbol{p}') d^3q, \tag{10}$$

where $S_\alpha(\boldsymbol{p})$ stands for the propagator of the open-flavour meson pair and the effective potential is depicted schematically in Fig. 1. Other components of the t matrix can be found algebraically once a solution for Eq. (10) is known.

It is important to emphasise that the original coupled-channel problem with the interaction potential (1) amounts to the inversion of the matrices as large as $(N_\text{e} + N_\text{in} + N_\text{p}) \times (N_\text{e} + N_\text{in} + N_\text{p})$ where,

Figure 1. The full effective interaction potential in the elastic channels. The thin solid lines, broad solid lines and dashed lines denote heavy-light mesons, heavy mesons, and light mesons, respectively, and the double line denotes the pole term propagator G_0. Potentials $V_{\alpha a}$ and $V_{b\beta}$ are defined in Eqs. (7) and (8).

while both $N_{\rm p}$ and $N_{\rm e}$ are expected to be of the order of unity, the number of the inelastic channels can be quite large, $N_{\rm in} \gg 1$. Since the fitting procedure amounts to multiple matrix inversions of this kind the problem of the data analysis becomes not feasible. In the meantime, the resulting effective equation (10) contains as small matrices as $N_{\rm e} \times N_{\rm e}$ while the other components of the t matrix refer to the matrices of the size $N_{\rm p} \times N_{\rm p}$—see the details in Refs. [7, 8]. In either case the rank of the matrices to be inverted can hardly exceed 2. Such a dramatic reduction of the rank of the matrices involved is crucially important for the practical parametrisation which will be discussed in the next section.

Another important property of the solution found is that the inelastic channels enter the problem as a sum, that is adding a new inelastic channel to the system does not entail starting the entire procedure from scratch but instead only amounts to minor changes in the sum of the inelastic loops.

Finally, once unitarity is preserved at every step of the procedure employed then the coupled-channel system used for the data analysis can be straightforwardly checked for selfconsistency. Indeed, if an additional inelasticity artificially added to the system is required to provide a good overall fit for the data analysed then the coupled-channel problem is incomplete and extra inelastic channels need to be measured and incorporated into the system.

The main source of information about resonances is provided by production reactions. The production amplitude from a point source into channel x (elastic or inelastic) reads

$$\mathcal{M}_x = -\sum_\beta \quad , \tag{11}$$

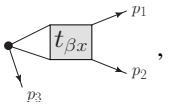

where the production source was assumed to be elastic (it also proves convenient to define the ratios of the sources ξ_α for $\alpha = 2, \ldots N_{\rm e}$) and the Born term was neglected compared to the rescattering term. This is justified since, for the cases of interest, the rescattering terms give the dominant contribution to the amplitude due to the presence of near-threshold poles. Also, for simplicity, the final-state interaction of the spectator particle 3 with the rest of the system is neglected. Further details of the formalism and the relevant formulae can be found in Refs. [7, 8].

3 Practical parametrisation

In order to proceed from the general solution of the coupled-channel Lippmann-Schwinger equations discussed in the previous section to a practical parametrisation for the line shapes we first simplify the interaction matrix (1) and take it in the form

$$\hat{V} = \begin{array}{c} \begin{matrix} b = \overline{1, N_p} & \beta = \overline{1, N_e} & i = \overline{1, N_{in}} \end{matrix} \\ \begin{pmatrix} v_{ab} & v_{a\beta} & \lambda_i (k_i^{in})^{l_i} \\ v_{\alpha b} & v_{\alpha\beta} & g_{i\alpha} (k_i^{in})^{l_i} \\ \lambda_j (k_j^{in})^{l_j} & g_{j\beta} (k_j^{in})^{l_j} & 0 \end{pmatrix} \end{array} \begin{matrix} a = \overline{1, N_p} \\ \alpha = \overline{1, N_e} \\ j = \overline{1, N_{in}}\,, \end{matrix} \tag{12}$$

where k_i^{in} is the momentum in the i-th inelastic channel in the final state while all elastic channels are assumed to be in the S wave, so that all other entries in $\hat{V}$, *cf.* Eq. (12), are treated as constant coupling constants. In addition, it is assumed that the solution of the Lippmann-Schwinger equation

$$t^v_{\alpha\beta}(\boldsymbol{p},\boldsymbol{p}') = v_{\alpha\beta}(\boldsymbol{p},\boldsymbol{p}') - \sum_{\gamma=1}^{N_c}\int v_{\alpha\gamma}(\boldsymbol{p},\boldsymbol{q})S_\gamma(\boldsymbol{q})t^v_{\gamma\beta}(\boldsymbol{q},\boldsymbol{p}')d^3q \tag{13}$$

for the direct elastic interaction is parametrised in a suitable form [8–10].

The most general form of the parametrisation derived for the coupled-channel problem (12) is discussed in detail in Refs. [7, 8]. In what follows a simplified version of such a parametrisation will be used which is suitable for the data analysis for the 1^{+-} isovector states $Z_b(10610)$ and $Z_b(10650)$ found recently by the Belle Collaboration. The existing experimental data for the Z_b's are exhausted by 7 decay chains [11–13]:

$$\begin{gathered}\Upsilon(5S)\to\pi Z_b^{(\prime)}\to\pi B^{(*)}\bar{B}^*,\\ \Upsilon(5S)\to\pi Z_b^{(\prime)}\to\pi\pi\Upsilon(nS),\quad n=1,2,3,\\ \Upsilon(5S)\to\pi Z_b^{(\prime)}\to\pi\pi h_b(mP),\quad m=1,2.\end{gathered}\tag{14}$$

Since the $Z_b^{(\prime)}$ states are isovectors which contain a $b\bar{b}$ pair then their minimal quark contents is four-quark, that is these states are inevitably exotic. The bare pole terms for such states would correspond to tetraquarks which we do not consider at this stage—they should only be added to the system if the simplest form of the equations, without tetraquarks, fails to describe the data well enough. Therefore, in the potential matrix (12) above only the couplings $v_{\alpha\beta}$ and $g_{i\alpha}$ are retained while all others are set to zero.

It is also important to notice that the b quark is heavy, $m_b \gg \Lambda_{\rm QCD}$, so that the b-quark spin decouples from the system. This results in the Heavy Quark Spin Symmetry (HQSS) which allows one to impose various constraints on the parameters of the equations. In particular, the C-odd combinations of the $B^{(*)}$ and B^* mesons are [14, 15]

$$|B\bar{B}^*\rangle_{1^{+-}} = -\frac{1}{\sqrt{2}}\Big[(1^-_{\bar{b}b}\otimes 0^-_{\bar{q}q})_{S=1} + (0^-_{\bar{b}b}\otimes 1^-_{\bar{q}q})_{S=1}\Big], \tag{15}$$

$$|B^*\bar{B}^*\rangle_{1^{+-}} = \frac{1}{\sqrt{2}}\Big[(1^-_{\bar{b}b}\otimes 0^-_{\bar{q}q})_{S=1} - (0^-_{\bar{b}b}\otimes 1^-_{\bar{q}q})_{S=1}\Big], \tag{16}$$

where $J^-_{\bar{b}b}$ and $J^-_{\bar{q}q}$ denote the spin wave function of the bottomonium and the light-quark pair, respectively. It is easy to see that if the HQSS is assumed to be exact then the couplings $g_{i\alpha}$—see Eq. (12)—are subject to the constraints following from Eqs. (15) and (16), namely,

$$\frac{g_{[\pi\Upsilon(nS)][B^*\bar{B}^*]}}{g_{[\pi\Upsilon(nS)][B\bar{B}^*]}} = -1,\quad \frac{g_{[\pi h_b(mP)][B^*\bar{B}^*]}}{g_{[\pi h_b(mP)][B\bar{B}^*]}} = 1,\quad \xi = \frac{g_{[\pi\Upsilon(5S)][B^*\bar{B}^*]}}{g_{[\pi\Upsilon(5S)][B\bar{B}^*]}} = -1, \tag{17}$$

where $n = 1, 2, 3$ and $m = 1, 2$ and, in addition, it was used that the elastic channels $B\bar{B}^*$ and $B^*\bar{B}^*$ are produced in the decays of the $\Upsilon(5S)$ bottomonium—see Eq. (14)—so that the ratio of the sources ξ is also subject to the same heavy-quark constraint.

In addition, the HQSS implies that the direct interaction potential takes the form

$$v(1^{+-}) = \begin{pmatrix} V_{B\bar{B}^*\to B\bar{B}^*} & V_{B\bar{B}^*\to B^*\bar{B}^*}\\ V_{B^*\bar{B}^*\to B\bar{B}^*} & V_{B^*\bar{B}^*\to B^*\bar{B}^*}\end{pmatrix} = \frac{1}{2}\frac{1}{(2\pi)^2\mu}\begin{pmatrix}\gamma_s^{-1}+\gamma_t^{-1} & \gamma_s^{-1}-\gamma_t^{-1}\\ \gamma_s^{-1}-\gamma_t^{-1} & \gamma_s^{-1}+\gamma_t^{-1}\end{pmatrix}, \tag{18}$$

where the subscript of the parameters γ_s and γ_t corresponds to the singlet and triplet state of the heavy-quark pair, respectively. For simplicity, we do not distinguish between the reduced masses in the $B\bar{B}^*$ and $B^{(*)}\bar{B}^*$ systems and set them both equal to μ. The t matrix—solution of the Lippmann-Schwinger equation (13) in the elastic channels $B^{(*)}\bar{B}^*$ takes the form [7, 8]

$$t^v = \frac{1}{(2\pi)^2\mu}\frac{1}{\mathrm{Det}}\begin{pmatrix} \frac{1}{2}(\gamma_s+\gamma_t)+ik_{B^*\bar{B}^*} & \frac{1}{2}(\gamma_t-\gamma_s) \\ \frac{1}{2}(\gamma_t-\gamma_s) & \frac{1}{2}(\gamma_s+\gamma_t)+ik_{B\bar{B}^*} \end{pmatrix}, \tag{19}$$

with

$$\mathrm{Det} = \gamma_s\gamma_t - k_{B\bar{B}^*}k_{B^*\bar{B}^*} + \frac{i}{2}(\gamma_s+\gamma_t)(k_{B\bar{B}^*}+k_{B^*\bar{B}^*}), \tag{20}$$

where $k_{B\bar{B}^*}$ and $k_{B^*\bar{B}^*}$ are the momenta in the channels $B\bar{B}^*$ and $B^*\bar{B}^*$, respectively.

Then the solution $t_{\alpha\beta}$ ($\alpha,\beta = 1,2$) of the Lippmann-Schwinger Eq. (10) with the full effective elastic potential can be built using the general formulae derived in Refs. [7, 8] and the differential production rates in the elastic and inelastic channels read

$$\frac{d\mathrm{Br}[B\bar{B}^*]}{dM} = \mathcal{N}_{B\bar{B}^*}\left|t_{11}+\xi t_{21}\right|^2 p_\pi k_{B\bar{B}^*}, \tag{21}$$

$$\frac{d\mathrm{Br}[B^*\bar{B}^*]}{dM} = \mathcal{N}_{B^*\bar{B}^*}\left|t_{12}+\xi t_{22}\right|^2 p_\pi k_{B^*\bar{B}^*}, \tag{22}$$

$$\frac{d\mathrm{Br}[\pi\Upsilon(nS)]}{dM} = \mathcal{N}_{\pi\Upsilon(nS)}\left|(t_{11}+\xi t_{21}) + \frac{g_{[B^*\bar{B}^*][\pi\Upsilon(nS)]}}{g_{[B\bar{B}^*][\pi\Upsilon(nS)]}}(t_{12}+\xi t_{22})\right|^2 p_\pi k_{\pi\Upsilon(nS)}, \quad n=1,2,3 \tag{23}$$

$$\frac{d\mathrm{Br}[\pi h_b(mP)]}{dM} = \mathcal{N}_{\pi h_b(mP)}\left|(t_{11}+\xi t_{21}) + \frac{g_{[B^*\bar{B}^*][\pi h_b(mP)]}}{g_{[B\bar{B}^*][\pi h_b(mP)]}}(t_{12}+\xi t_{22})\right|^2 p_\pi k^3_{\pi h_b(mP)}, \quad m=1,2, \tag{24}$$

where M varies in the range from $M_{\min} = m_1 + m_2$ (the subscript 1 and 2 numerates the particles in the final states $B\bar{B}^*$, $B^*\bar{B}^*$, $\pi\Upsilon(nS)$, and $\pi h_b(mP)$) to $M_{\max} = M_{\mathrm{tot}} - m_\pi$ and p_π is the momentum of the spectator pion.

The total number of parameters which define the line shapes in 7 channel (21)-(24) equals to 20—see Refs. [7, 8] for their detailed description. Meanwhile, if the HQSS constrains (17) are applied then the number of parameters is reduced to 14: 7 parameters define the overall norms in 7 distributions and 7 additional parameters,

$$\gamma_s, \quad \gamma_t, \quad g_{[\pi h_b(1P)][B\bar{B}^*]}, \quad g_{[\pi h_b(2P)][B\bar{B}^*]}, \quad g_{[\pi\Upsilon(1S)][B\bar{B}^*]}, \quad g_{[\pi\Upsilon(2S)][B\bar{B}^*]}, \quad g_{[\pi\Upsilon(3S)][B\bar{B}^*]}, \tag{25}$$

totally fix all 7 line shapes. It should be noticed that, if a naive sum of two Breit-Wigners had been used in each channel, the number of parameters would have been a few times larger.

4 Fits for the data and the nature of the Z_b's

With the practical parametrisation derived in the previous section we are in a position to perform a combined data analysis for the 7 channels (14). As an experimental input we use

- background-subtracted and efficiency-corrected distributions in M for the $B^{(*)}\bar{B}^*$ and $\pi h_b(nP)$ channels [11, 13] with floating normalisation in each channel. Notice that for the $B^{(*)}\bar{B}^*$ channels the old data [16] and the preliminary new data [17] were used in Ref. [7] and Ref. [8], respectively;
- ratios of the total branching fractions [11, 12, 16, 18] for all five inelastic channels $\pi\Upsilon(nS)$ and $\pi h_b(mP)$ with $n = 1,2,3$ and $m = 1,2$.

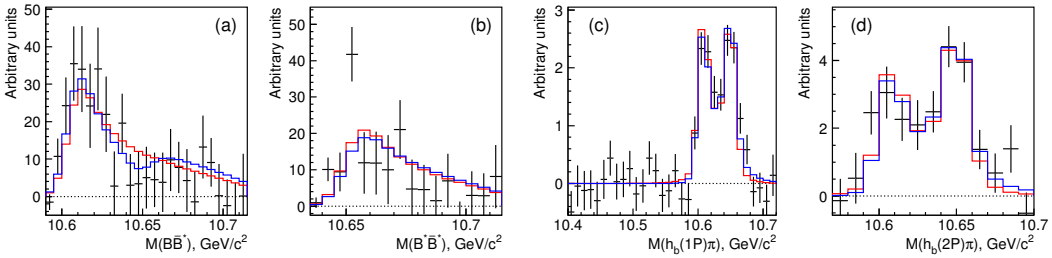

Figure 2. Fitted line shapes for the $Z_b(10610)$ and $Z_b(10650)$ in the channels $B^{(*)}\bar{B}^*$ and $\pi h_b(mP)$ ($m = 1, 2$).

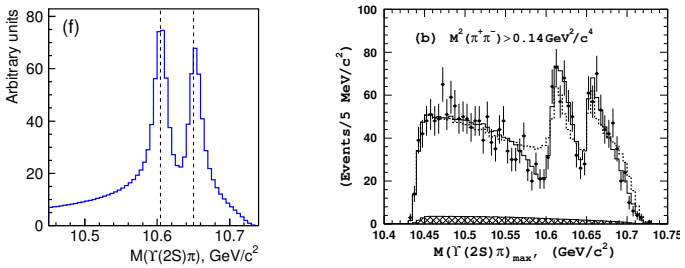

Figure 3. Predicted line shapes of the $Z_b(10610)$ and $Z_b(10650)$ in the $\pi\Upsilon(2S)$ channel for fit B. To guide the eye, as the last plot, we also show the corresponding experimental figure adapted from Ref. [12]. Notice that the behaviour of the line shape below the left shoulder of the lower peak is influenced by the effects which lie beyond the scope of the present research and will be addressed in future publications. Notice also that the presence of the nonresonant background in the experimental figure does not allow its direct comparison with the predicted line shapes.

We do not use the information on the $Z_b^{(\prime)}$ line shapes in the $\pi\Upsilon(nS)$ channels, since in the one-dimensional fit it is not possible to correctly take into account the interference with the nonresonant continuum, which is significant in the $\Upsilon(5S) \to \pi^+\pi^-\Upsilon(nS)$ transitions. Therefore, the line shapes in the $\pi\Upsilon(nS)$ channels come out as predictions of the approach.

We consider two types of fits: in fit A all parameters are totally unconstrained (as a matter of fact, since the line shapes in the $\pi\Upsilon(nS)$ channels are not fitted and therefore the ratios of the couplings for these channels cannot be extracted reliably then the ratios $g_{[\pi\Upsilon(nS)][B^*\bar{B}^*]}/g_{[\pi\Upsilon(nS)][B\bar{B}^*]} = -1$ are artificially fixed in fit A for $n = 1, 2, 3$) while in fit B all HQSS constraints (17) are applied. Parameters of the fits are listed in Table 1 and the corresponding line shapes in comparison to the experimental data are shown in Fig. 2. The predicted line shape in the channel $\pi\Upsilon(2S)$ and the experimental plot for the same channel adapted from Ref. [12] are given in Fig. 3. Line shapes in the channels $\pi\Upsilon(1S)$ and $\pi\Upsilon(3S)$ look similar and are not shown.

One can make several conclusions from Table 1 and Fig. 2:

- Both fits A and B provide equally good description of the data.
- The pole positions in the energy complex plane which correspond to the Z_b's are similar in both fits which is a consequence of the nearly identical description of the data by the two fits mentioned above.

Table 1. Parameters of the fits A and B. Parameters of fit B market with asterix are fixed from the HQSS.

Fit	Colour in Fig. 2	γ_s, MeV	γ_t, MeV	ξ	$\frac{g_{[\pi h_b(1P)][B^*\bar{B}^*]}}{g_{[\pi h_b(1P)][B\bar{B}^*]}}$	$\frac{g_{[\pi h_b(2P)][B^*\bar{B}^*]}}{g_{[\pi h_b(2P)][B\bar{B}^*]}}$	C.L.
A	Blue	43^{+37}_{-58}	-211^{+68}_{-58}	-0.80 ± 0.10	$1.8^{+0.9}_{-0.5}$	$1.8^{+0.9}_{-0.5}$	53%
B	Red	-70^{+32}_{-36}	-83^{+35}_{-38}	-1	1	1	48%

- Both Z_b states are virtual states located on the unphysical Riemann sheets just below the respective thresholds, with "binding energies" defined as

$$\varepsilon_B(Z_b) \equiv M(B\bar{B}^*) - M(Z_b), \quad \varepsilon_B(Z_b') \equiv M(B^*\bar{B}^*) - M(Z_b'), \tag{26}$$

  which equal to

$$\varepsilon_B(Z_b) = (1.10^{+0.79}_{-0.54} \pm i0.06^{+0.02}_{-0.02})\ \text{MeV}, \quad \varepsilon_B(Z_b') = (1.10^{+0.79}_{-0.53} \pm i0.08^{+0.03}_{-0.05})\ \text{MeV}, \tag{27}$$

  for the parameters of fit C, and

$$\varepsilon_B(Z_b) = (0.60^{+1.40}_{-0.49} \pm i0.02^{+0.02}_{-0.01})\ \text{MeV}, \quad \varepsilon_B(Z_b') = (0.97^{+1.42}_{-0.68} \pm i0.84^{+0.22}_{-0.34})\ \text{MeV}, \tag{28}$$

  for the parameters of fit D.
- Since quark systems bound by the confinement can only be bound states, the nature of the Z_b's extracted from the fits argues in favour of a large hadronic component in their wave functions. Furthermore, as was claimed above, the data are well described under the assumption of no quark component in the wave functions at all.
- The unconstrained fit A for the updated data in the elastic channels [13] is marginally compatible with the HQSS which is to be confronted with the largely broken HQSS in the fits to the old data [16]—see Ref. [7]. It is expected that even better data will clarify the amount of HQSS breaking in the Z_b systems.
- Although both fits describe the data well and predict the same nature of the Z_b's, the present quality of the data does not allow one to fix the parameters of the fits reliably—see Table 1 for the substantial different in the parameters γ_s and γ_t in fits A and B. More accurate data and/or inclusion of the information for the $\pi\Upsilon(nS)$ channels to the combined fit are expected to improve the sitution.
- It follows from Eq. (18) that for $\gamma_s \simeq \gamma_t$ the off-diagonal terms of the potential matrix vanish, so that transitions between different elastic channels are strongly suppressed. This situation is realised in the constrained fit B—see Table 1—and, as a result, the line shape in the $B\bar{B}^*$ channel demonstrates a much more tamed behaviour near the $B^*\bar{B}^*$ threshold as compared to the curve for fit A in which a well pronounced peak is formed in this region—see the first plot in Fig. 2.
- Since in the strict HQSS limit the flip of the b-quark spin is forbidden, the absence of the transitions between the $B\bar{B}^*$ and $B^*\bar{B}^*$ channels is equivalent to the conservation of the light-quark spin as well. The idea of the Light-Quark Spin Symmetry responsible for this additional conservation law was put forward in Ref. [19]. Meanwhile, it remains to be seen what kind of underlying mechanisms could result in such a symmetry.

5 Conclusions

In this work we demonstrated that using a coupled-channels model supplied with quite a few natural assumptions results in a simple but phenomenologically adequate parametrisation for the line shape

which appears to be well suited for the combined data analysis for all production and decay modes of the given near-threshold resonance or a system of resonances in the spectrum of heavy quarkonia.

All parameters used possess a clear physical interpretation which provides a way to remove the gap between theory and experiment, since microscopic or first-principle calculations can now be used to explain the values of the parameters (the coupling constants in the first place) extracted from the fit for the data rather than to reproduce the experimental data points themselves.

In the suggested approach unitarity is preserved at every stage. In particular, this implies that if a good fit for the existing data requires an additional inelasticity then the data set is incomplete and the basis of the coupled-channel model needs to be extended.

The practical parametrisation which emerges can be quite straightforwardly generalised in order to extend the basis of the coupled channels, to implement constraints from various symmetries, and to incorporate any additional information provided by complementary approaches, for example, by the numerical calculations on the lattice.

Further developments of the approach should include the final-state interaction in the system, for example, by combining the present approach with the formalism outlined in Ref. [20], the pion exchange between the constituents as well as additional production mechanisms. They will be subject of future publications.

This work is supported in part by the DFG and the NSFC through funds provided to the Sino-German CRC 110 “Symmetries and the Emergence of Structure in QCD” (NSFC Grant No. 11261130311). R. M. and A. N. acknowledge support from the Russian Science Foundation (Grant No. 15-12-30014). F.-K. G. is partially supported by the Thousand Talents Plan for Young Professionals.

References

[1] S. K. Choi *et al.* [Belle Collaboration], Phys. Rev. Lett. **91**, 262001 (2003).
[2] T. Abe *et al.* [Belle-II Collaboration], arXiv:1011.0352 [physics.ins-det].
[3] A. G. Drutskoy, F. K. Guo, F. J. Llanes-Estrada, A. V. Nefediev and J. M. Torres-Rincon, Eur. Phys. J. A **49**, 7 (2013).
[4] D. M. Asner *et al.*, Int. J. Mod. Phys. A **24**, S1 (2009).
[5] M. F. M. Lutz *et al.* [PANDA Collaboration], arXiv:0903.3905 [hep-ex].
[6] M. Cleven, F. K. Guo, C. Hanhart and U. G. Meißner, Eur. Phys. J. A **47**, 120 (2011).
[7] C. Hanhart, Y. S. Kalashnikova, P. Matuschek, R. V. Mizuk, A. V. Nefediev and Q. Wang, Phys. Rev. Lett. **115**, 202001 (2015).
[8] F.-K. Guo, C. Hanhart, Y. S. Kalashnikova, P. Matuschek, R. V. Mizuk, A. V. Nefediev, Q. Wang and J.-L. Wynen, Phys. Rev. D **93**, 074031 (2016).
[9] V. Baru, C. Hanhart, Y. S. Kalashnikova, A. E. Kudryavtsev and A. V. Nefediev, Eur. Phys. J. A **44**, 93 (2010).
[10] C. Hanhart, Y. S. Kalashnikova and A. V. Nefediev, Eur. Phys. J. A **47**, 101 (2011).
[11] A. Bondar *et al.* [Belle Collaboration], Phys. Rev. Lett. **108**, 122001 (2012).
[12] A. Garmash *et al.* [Belle Collaboration], Phys. Rev. D **91**, no. 7, 072003 (2015).
[13] A. Garmash *et al.* [Belle Collaboration], Phys. Rev. Lett. **116**, 212001 (2016).
[14] A. E. Bondar, A. Garmash, A. I. Milstein, R. Mizuk and M. B. Voloshin, Phys. Rev. D **84**, 054010 (2011).
[15] M. B. Voloshin, Phys. Rev. D **84**, 031502 (2011).

[16] I. Adachi *et al.* [Belle Collaboration], arXiv:1209.6450 [hep-ex].
[17] A. Bondar, *In Proceedings of of XXVII Int. Symp. on Lepton Photon Interactions at High Energies*, Lubljana, Slovenia, (2015).
[18] I. Adachi *et al.* [Belle Collaboration], Phys. Rev. Lett. **108**, 032001 (2012).
[19] M. B. Voloshin, Phys. Rev. D **93**, 074011 (2016).
[20] Y. H. Chen, J. T. Daub, F. K. Guo, B. Kubis, U. G. Meißner and B. S. Zou, Phys. Rev. D **93**, 034030 (2016).